Premières journées QGP-France

Etretat, France, 3-6 juillet 2006

Elliptic Flow in a Final State Interaction Model

Elena G. Ferreiro

Universidad de Santiago de Compostela, Spain

Contents:

1. **The model**
2. **Large p_T suppression**
3. **Elliptic flow**

hep-ph/0403081 with A. Capella, A. B. Kaidalov and D. Sousa
hep-ph/0602196 with A. Capella

INTRODUCTION

• RHIC data show azimuthal anisotropy in the production of particles in heavy ion collsions: **Elliptic Flow**

Interpretations

• **Hydrodynamical model: Signal of early thermalization $\Rightarrow$ QGP**

Particles tend to go in the direction of the strongest pressure gradients, hence preferably in the collision plan.

• **Final state interaction model: Jet absorption in dense matter**

Due to the asymmetry of the overlap region of the two nuclei, the average amount of matter traversed by a parton depends on its azimuthal direction with respect to the reaction plane, which leads to an azimuthal anisotropy of the emitted jets.

Our mechanism: Final state interactions in the whole p_T region
$\Rightarrow$ Large p_T suppression and elliptic flow

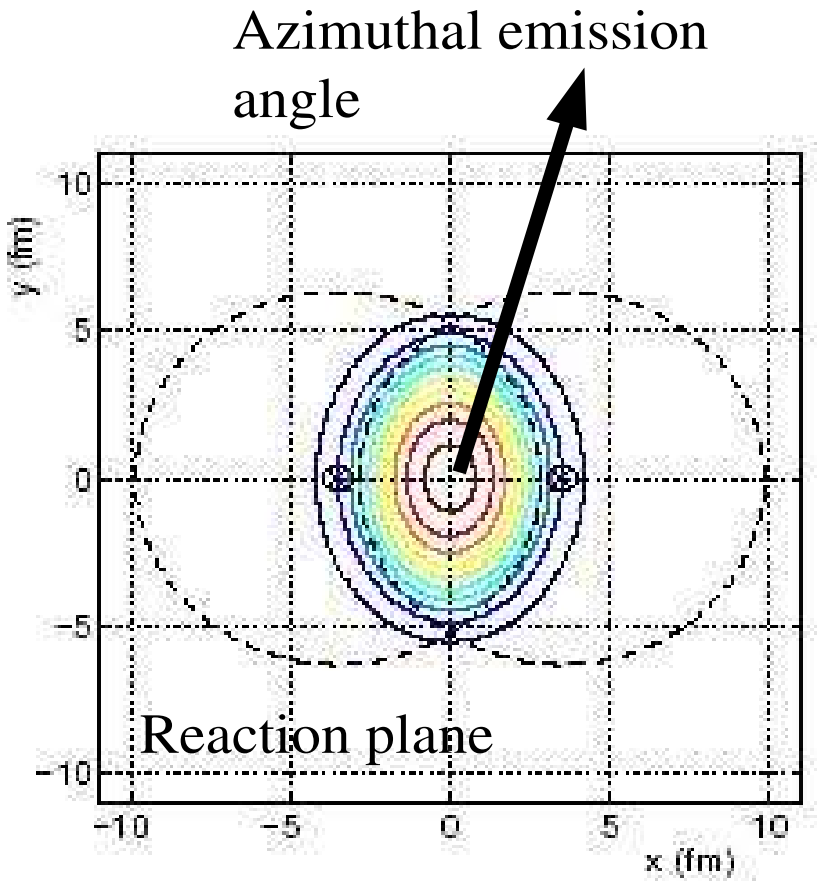

$$v_2 = \frac{< y^2 - x^2 >}{< y^2 + x^2 >}$$

In non-central heavy ion collisions, the geometrical overlap region has an almond shape in the transverse plane, with its short axis in the reaction plane

Elliptic Flow: momentum-space anisotropy, with more momentum flowing into the reaction plane than out of it

The momentum flow preferably into the *short* direction

Faster motion into the reaction plane than perpendicular to it

THE FINAL STATE INTERACTION MODEL

• The interaction of a particle or a parton with the medium is described by the gain and loss differential equations which govern final state interactions:

$$\tau \, \frac{d\rho_i}{d\tau} = \sum_{k,\ell} \sigma_{k\ell} \; \rho_k \; \rho_\ell - \sum_k \sigma_{ik} \; \rho_i \; \rho_k$$

$\rho_i \equiv dN^{AA \to i}(b)/dyd^2s =$ space-time densities

$\rho(\tau, y, s) \sim \frac{1}{\tau} \, \rho(y, s)$

Dilution on time of densities: isoentropic longitudinal expansion, no transverse expansion

$\sigma_{ij} =$ interaction cross-sections

longitudinal proper time τ, space-time rapidity y, transverse coordinate s

• The first term describes the **gain** in type i particle yield resulting from the interaction of k and ℓ.

• The second one corresponds to the **loss** of type i particles resulting from its interaction with particle k.

Derivation of the suppression factor

• Consider a π^0 produced at fixed p_T interacting with the medium

• In the interaction, with cross-section σ, the π^0 suffers a decrease in its transverse momentum with a p_T-shift δp_T $\quad$ $-energy\ loss-$

$\Rightarrow$ A loss in the π^0 yield in a given p_T bin

$\Rightarrow$ A gain resulting from π^0's produced at $p_T + \delta p_T$

Gain and loss diferential equation for pions:

$$\tau \frac{d\rho_{\pi^0}}{d\tau} = -\sigma\ \rho_{medium}\ \rho_{\pi^0}(b, s, y, p_T) + \sigma\ \rho_{medium}\ \rho_{\pi^0}(b, s, y, p_T + \delta p_T)$$

• Steep fall-off of the p_T spectrum: the loss is larger than the gain
$\Rightarrow$ Net suppression of the π^0 yield at a given p_T

• Our equations have to be integrated between initial time τ_0 and freeze-out time τ_f.

• The solution depends only on the ratio τ_f/τ_0.

• We use the inverse proportionality between proper time and densities, $\tau_f/\tau_0 = \rho(b,s,y)/\rho_{pp}(y)$

$\rho_{pp}(y)$= density per unit rapidity for mb pp collisions at $\sqrt{s} = 200$ GeV= 2.24 fm^{-2}

$\rho(b,s,y)$ = density produced in the primary collisions

• Our densities can be either hadrons or partons:

At early times: densities are very high and hadrons not yet formed.
$\Rightarrow$ Our equations describe final state interactions at a partonic level.

At later times: we have interactions of full fledged hadrons.

σ represents an effective cross-section averaged over the interaction time

• Integrating

$$\tau \frac{d\rho_{\pi^0}}{d\tau} = -\sigma \ \rho(b,y) \left[\rho_{\pi^0}(b,y,p_T) - \rho_{\pi^0}(b,y,p_T+\delta p_T)\right]$$

from τ_0 to τ_f and taking $\rho(b,y,p_T)_{\pi^0} = dN_{\pi^0}/dbdydp_T$

• We obtain the suppression factor $S_{\pi^0}(b,y,p_T)$ of the yield of π^0's at given p_T due to its interaction with the dense medium:

$$\boxed{S_{\pi^0}(y,p_T,b) = \exp\left\{-\sigma \ \rho(b,y) \left[1 - \frac{N_{\pi^0}(p_T+\delta p_T)}{N_{\pi^0}(p_T)}(b)\right] \ \ell n \left(\frac{\rho(b,y)}{\rho_{pp}(y)}\right)\right\}}$$

With $\delta p_T \to \infty$: the gain term vanishes $\Rightarrow$ The survival probability has the same expression as in the case of J/ψ suppression without $c\bar{c}$ recombination.

With $\delta p_T = 0$: the loss and gain terms are identical $\Rightarrow$ The survival probability is equal to one.

Numerical results

To perform numerical calculations, we need the p_T **distribution** of the π^0's

- Value $R^0_{AA}(b, p_T)$ in the absence of final state interactions:

$$R^0_{AA}(b, p_T) = R^0_{AA}(b, p_T = 0) \left(\frac{p_T + p_0^{AA}(b)}{p_T + p_0^{pp}} \right)^{-n} \Bigg/ \left(\frac{p_0^{AA}(b)}{p_0^{pp}} \right)^{-n}$$

where $p_0(b) = (n-3)/2 < p_T >_b$, $n = 9.99$ and $< p_T >_b$ is the experimental value of $< p_T >$ at each b

- We have also tried different parametrizations for $R^0_{AA}(b, p_T)$:

Our final result depends little on the form of R^0_{AA} taking a p_T-shift $\delta p_T = p_T^\alpha / C$

To the value R^0_{AA} we apply the correction due to the suppression factor S_{π^0}

$$S_{\pi^0(b,p_T)}=\exp\left\{-\sigma\rho(b,y)\left[1-\frac{N_{\pi^0}(p_T+\delta p_T)}{N_{\pi^0}(p_T)}\right]\ell n\left(\frac{\rho(b,y)}{\rho_{pp}(y)}\right)\right\}$$

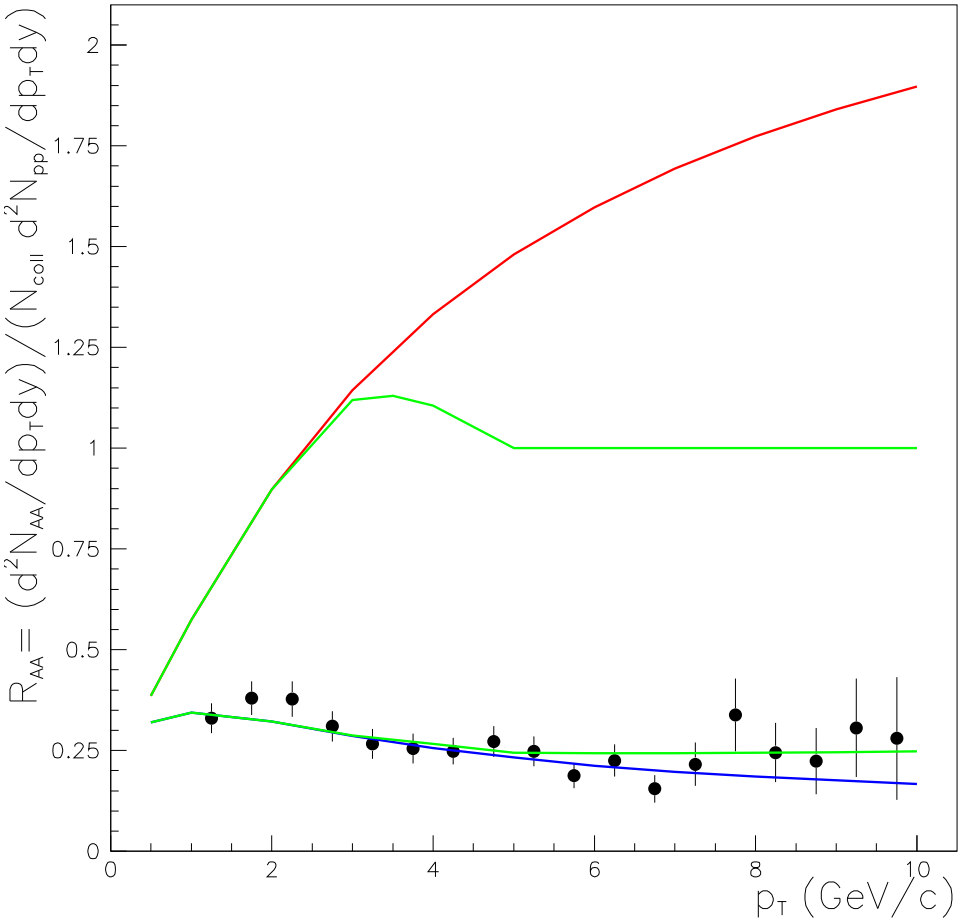

$$R_{AA}=R^0_{AA}(b,p_T)S_{\pi^0}(b,p_T)$$

$$\delta p_T = p_T^{3/2}/(20\ \mathrm{GeV}^{1/2})$$

$$R_{AA}=R^0_{AA}(b,p_T)\ S_{\pi^0}(b,p_T)$$

For $p_T \geq 5$ GeV:

$$R^0_{AA}(b,p_T \geq 5\ \mathrm{GeV}) = 1$$

$$\delta p_T = p_T^{0.8}/(9.5\ \mathrm{GeV}^{1/2})$$

R_{AA} CENTRALITY DEPENDENCE

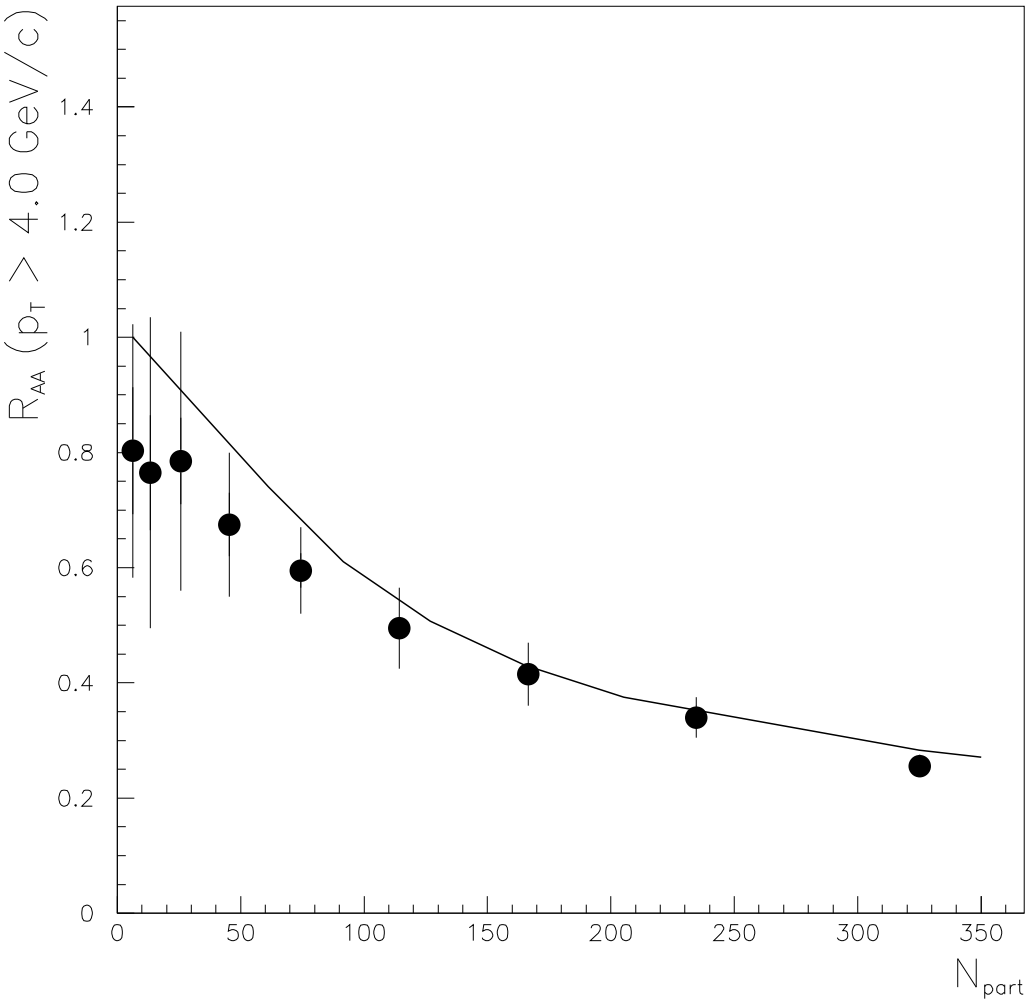

Centrality dependence of $R^{\pi^0}_{AuAu}$ for $p_T > 4$ GeV/c using the p_T shift $\delta p_T = p_T^{1.5}/20$. The data are from PHENIX.

ELLIPTIC FLOW

• Our final state interaction model takes into account the longitudinal expansion – with no consideration for the motion in the transverse plane.

• Elliptic flow, on the contrary, results from an asymmetry in the azimuthal angle ⇒ The motion in the transverse plane plays a fundamental role

• Extension of the model: **We take into account the different path length of the particles or partons in the transverse plane for each value of its azimuthal angle θ_R – measured with respect to the reaction plane.**

• At $y^* \sim 0$, **the path length** R_{θ_R}, measured from the center of the interaction region (overlap of the colliding nuclei) is given by

$$R_{\theta_R}(b) = R_A \frac{\sin(\theta_R - \alpha)}{\sin\theta_R}$$

where $R_A = 1.05\ A^{1/3}$ fm is the nuclear radius and $\sin\alpha = b\sin\theta_R/2R_A$.

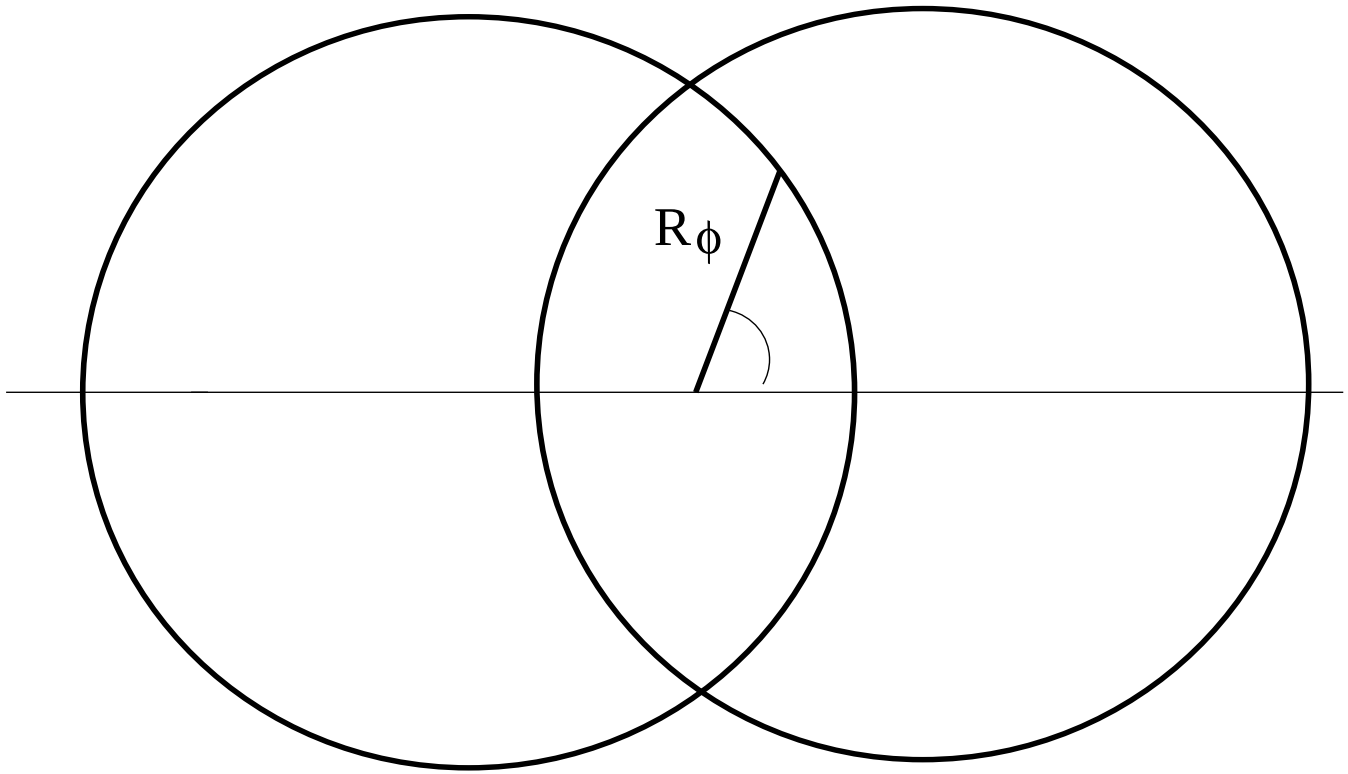
R_ϕ

Replacement:

$$\rho(b,y) \rightarrow \rho(b,y)\frac{R_{\theta_R}}{<R_{\theta_R}>}$$

$\Rightarrow$ Duration of the interaction and the density of the medium traversed by the particles: Proportional to the path length R_{θ_R} inside the overlap region of the colliding nuclei

Suppression factor:

$$S_{\pi^0}^{\theta_R}(p_T,b) = \exp\left\{-\sigma\rho(b,y)\frac{R_{\theta_R}}{<R_{\theta_R}>}\left[1-\frac{N_{\pi^0}(p_T+\delta p_T)}{N_{\pi^0}(p_T)}\right]\ell n\left(\frac{\rho(b,y)\frac{R_{\theta_R}}{<R_{\theta_R}>}}{\rho_{pp}(y)}\right)\right\}$$

Elliptic flow:

$$v_2(p_T,b) = \frac{\int_0^{90^\circ} d\theta_R \ \cos 2\theta_R \ S_{\pi^0}^{\theta_R}(p_T,b)}{\int_0^{90^\circ} d\theta_R \ S_{\pi^0}^{\theta_R}(p_T,b)}$$

$\theta_R = 0^\circ \Rightarrow$ Minimal path length and maximal survival probability

$\theta_R = 90^\circ \Rightarrow$ Maximal path length and minimal survival probability

v_2 TRANSVERSE MOMENTUM DEPENDENCE

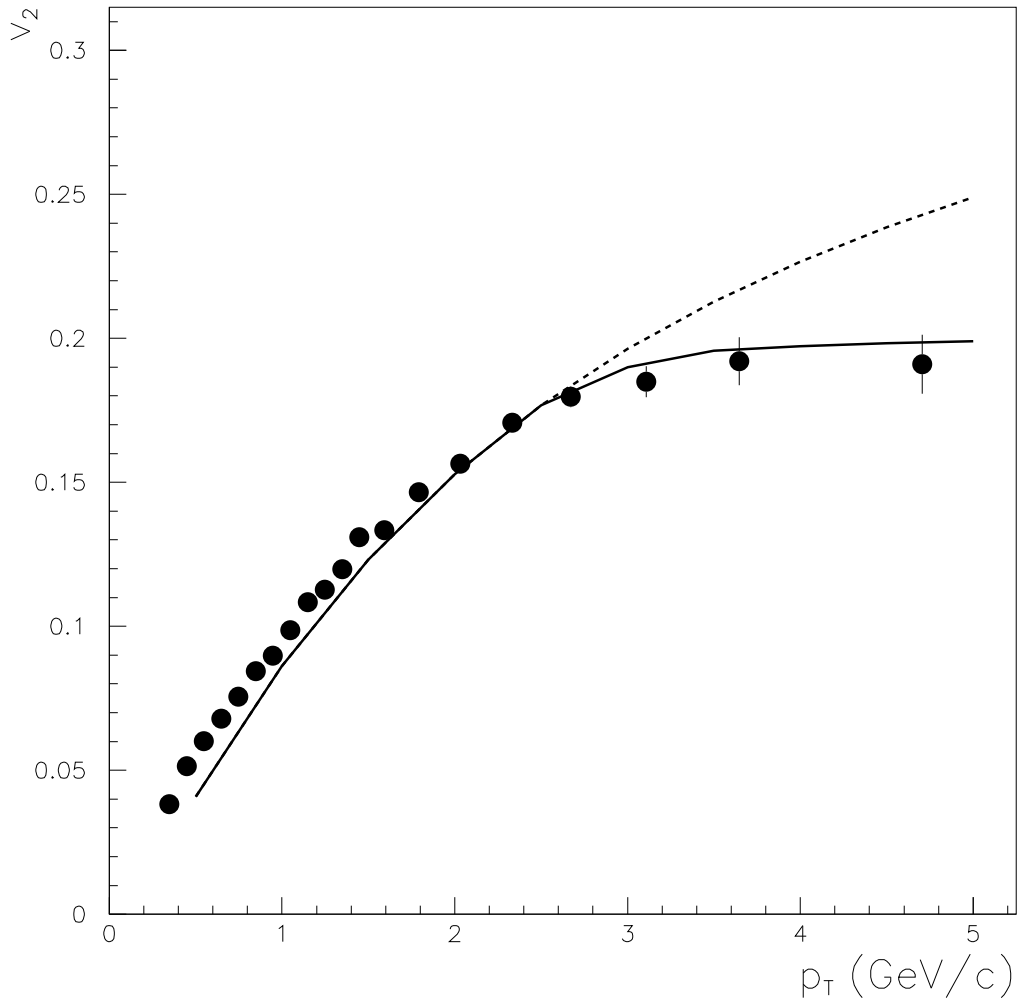

v_2 vs. p_T for charged hadrons in the centrality bin 13 %-26 %. Data: PHENIX

The dashed line: $\delta p_T = p_T^{3/2}/(20\ \mathrm{GeV}^{1/2})$.

The continous line: $\delta p_T = p_T^{0.8}/(9.5\ \ \mathrm{GeV}^{-0.2})$ for $p_T \geq 5$ GeV.

Hydrodynamics describes the v_2 data only in a small low-p_T interval

v_2 CENTRALITY DEPENDENCE

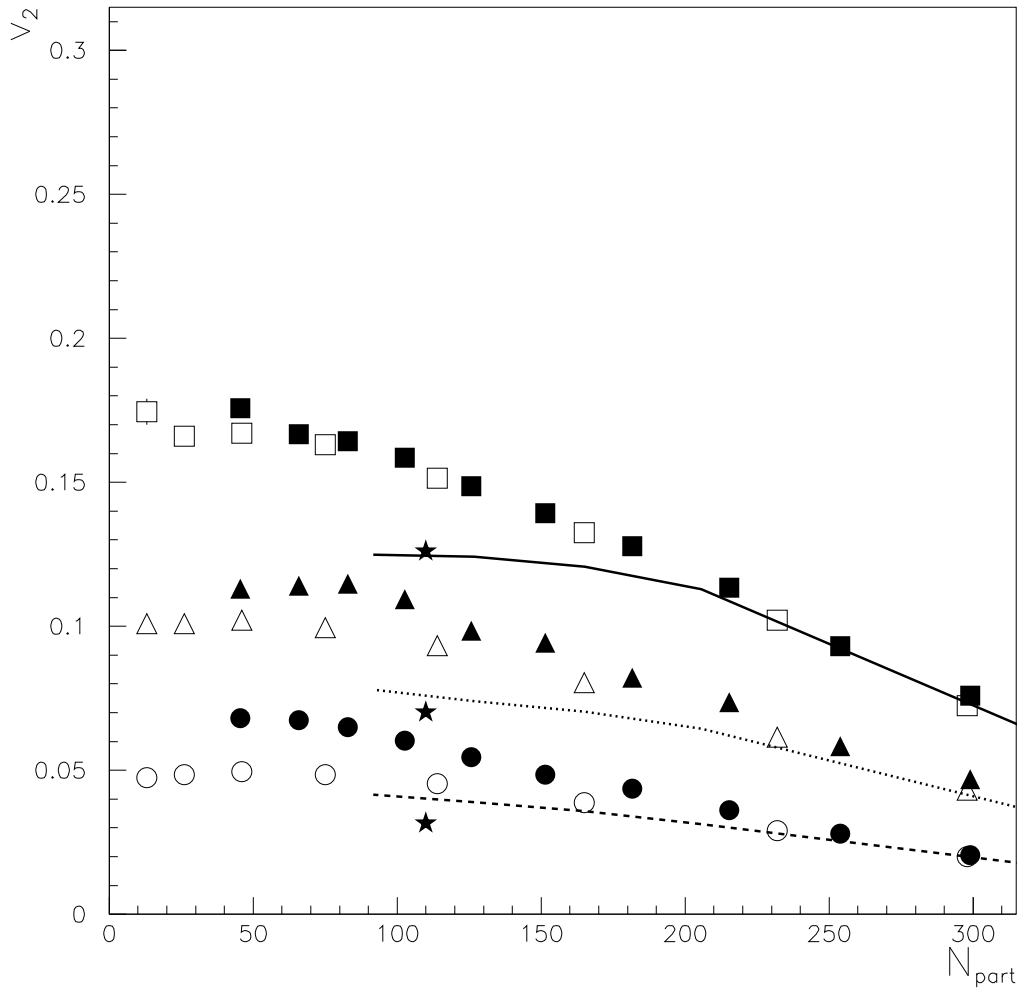

v_2 vs. the number of participants for charged hadrons

$p_T = 0.4$ GeV (lower line)

$p_T = 0.75$ Gev (middle)

$p_T = 1.35$ GeV (top)

Data: PHENIX (black), STAR (open)

3 experimental analysis:
reaction plane technique
cumulant analysis
correlation functions

Good agreement for central and medium collisions

Peripheral collisions?

R_{AA} AZIMUTHAL ANGLE DEPENDENCE

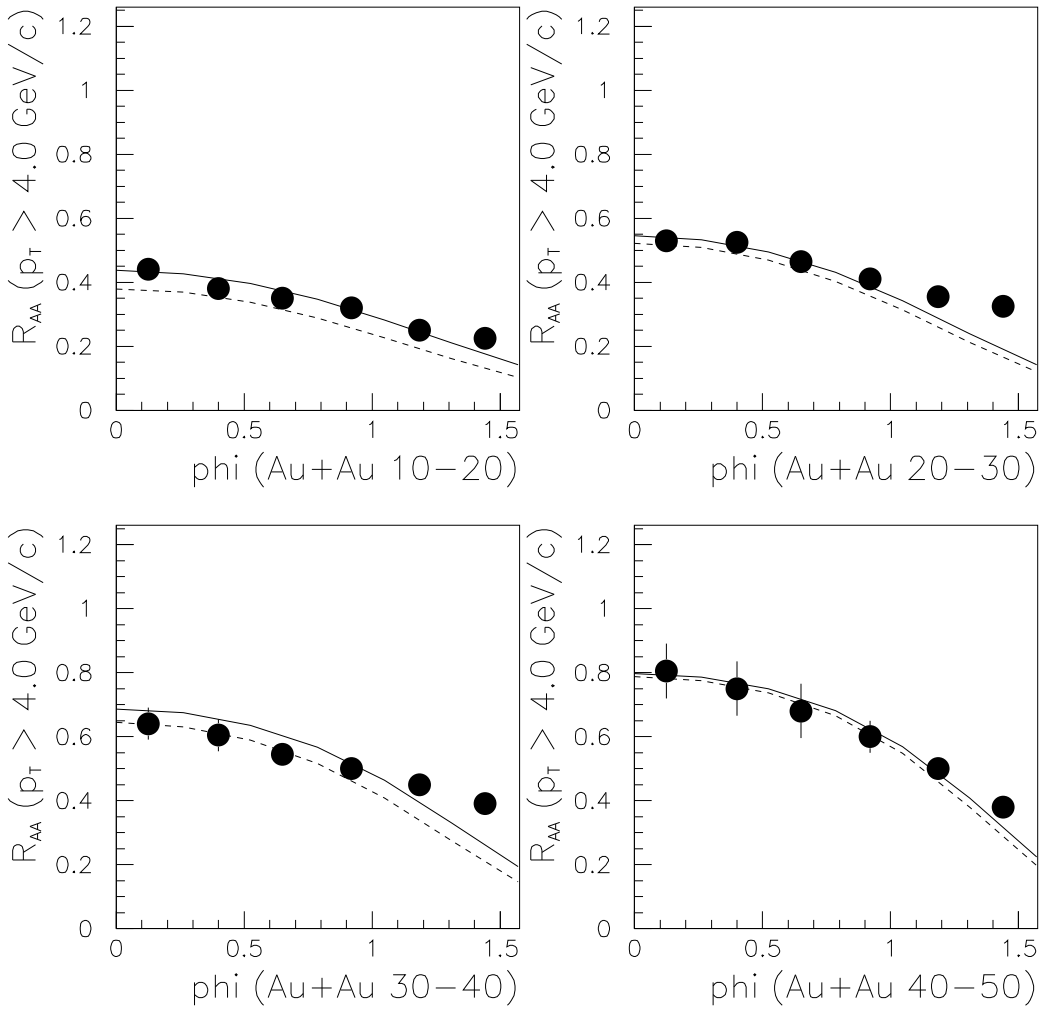

Values of the π^0 suppression $R_{AuAu}(b, \theta_R)$ as a function of the azimuthal angle θ_R for $p_T \geq 4$ GeV in various centrality bins. Data: PHENIX.

Peripheral collisions well reproduced

v_2 MASS DEPENDENCE

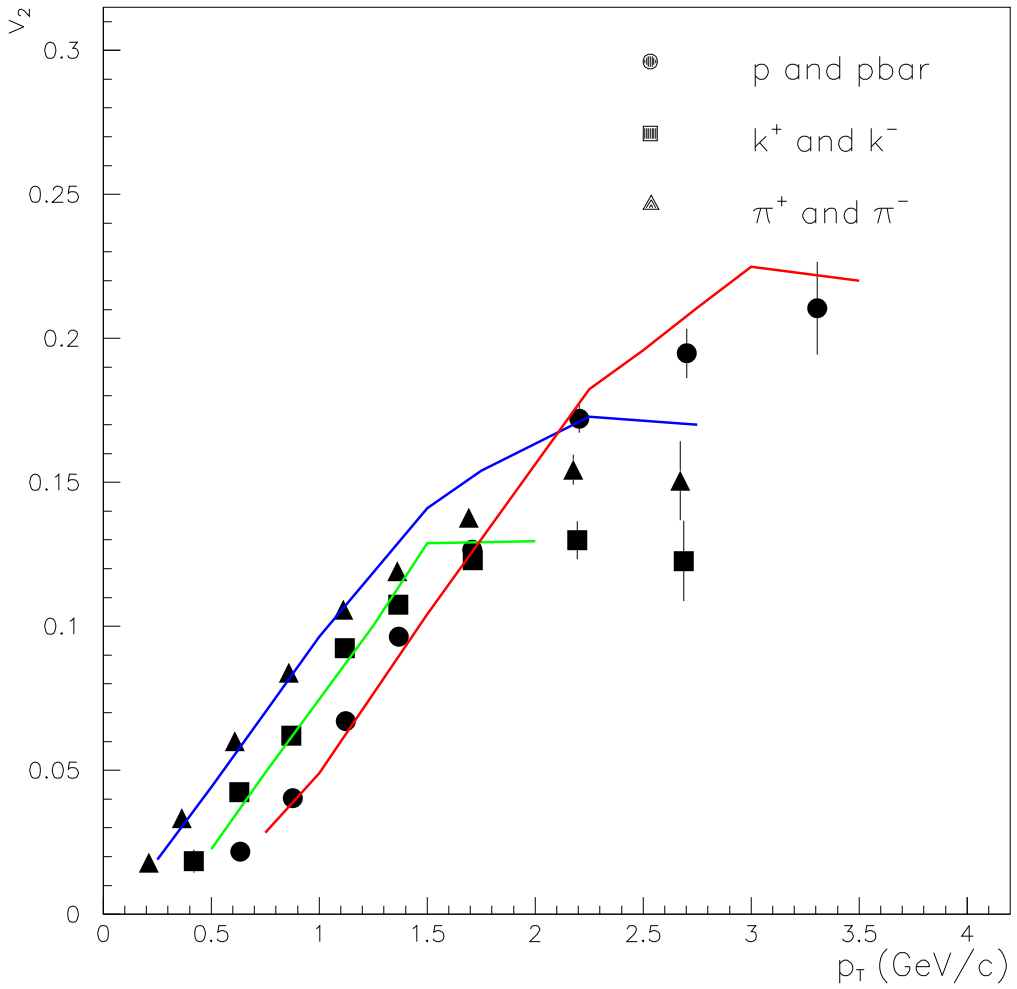

v_2 vs. p_T of differents particle species for minimun bias collisions

Data: PHENIX

v_2 of mesons falls below that of baryons for $p_T > 2$ GeV/c

Hydrodynamical model predicts the same mass ordering for v_2 at all p_T

CONCLUSIONS

At RHIC, different observations have appeared: strong suppression of high-p_T particles and large values of the elliptic flow at high p_T.

We have proposed a final state interaction model which takes into account the different path length of a particle in the transverse plane for each value of its azimuthal angle in the overlap area of the colliding nuclei.

In our approach, the mechanism responsible for the large p_T suppression does give a contribution to the elliptic flow: v_2 very close to the experimental ones are obtained in the whole p_T region, including the low p_T one.

Although this contribution to v_2 results from an asymmetry in the azimuthal angle, it can be qualified as non-flow: the mechanism from which it arises (fixed p_T suppression) is maximal at zero impact parameter and, moreover, thermalization is not needed.

We do not claim that the mechanism we have introduced gives the only contribution to the elliptic flow. In our opinion, our knowledge of the dynamics of the nuclear interaction is not sufficient to disentangle all the mechanisms and, therefore, to allow to draw clear-cut conclusions regarding the interpretation of the measured values of v_2.

DIFFICULTIES

Interaction-cross section identical for partons and hadrons

No realistic Woods-Saxons for the nuclear profile

Path-leght measured from de central point of the interaction

RADIAL FLOW

Radial flow: increase of the inverse slope T with the mass of the produced particle

$$T = T_0 + m < u_t >^2$$

T_0= freeze-out temperature, $< u_t >^2$= strength of the radial flow

Although $< u_t >^2$ increases with centrality, there is an effect in the most peripheral bin (60 - 92 %, $N_{part} = 14$) $\Rightarrow$ **Is a perfect fluid already produced at this low density?**

Is the origin of the T increase a genuine final state collective effect or is it contained in the initial state (Cronin effect, shadowing, etc.)?

$$\frac{d^2N}{2\pi m_T dm_T dy}(b) = \frac{1}{2\pi T(b)(T(b)+m_0))} A(b) \exp\left(-\frac{m_T - m_0}{T(b)}\right)$$

$$\frac{d^2N_i^{Initial}}{2\pi m_T dm_T dy}(b) = \frac{d^2N_i}{2\pi m_T dm_T dy}(b)/S_i(y, p_T, b)$$

The results for the initial p_T distribution obtained in this way are shown in Fig. 2 (full lines). The resulting values of the initial inverse slope $T^{Initial}$ for the various types of particle, in three centrality bins, is given in Fig. 1. We see that the inverse slopes of the initial p_T-distributions are larger than the measured ones and their differences increase with centrality. We also see that the "radial flow", i.e. the increase of T with mass is already present in the initial condition. Actually, the slope $< u_t >^2$ of the mass dependence is larger in the initial condition than in the data.

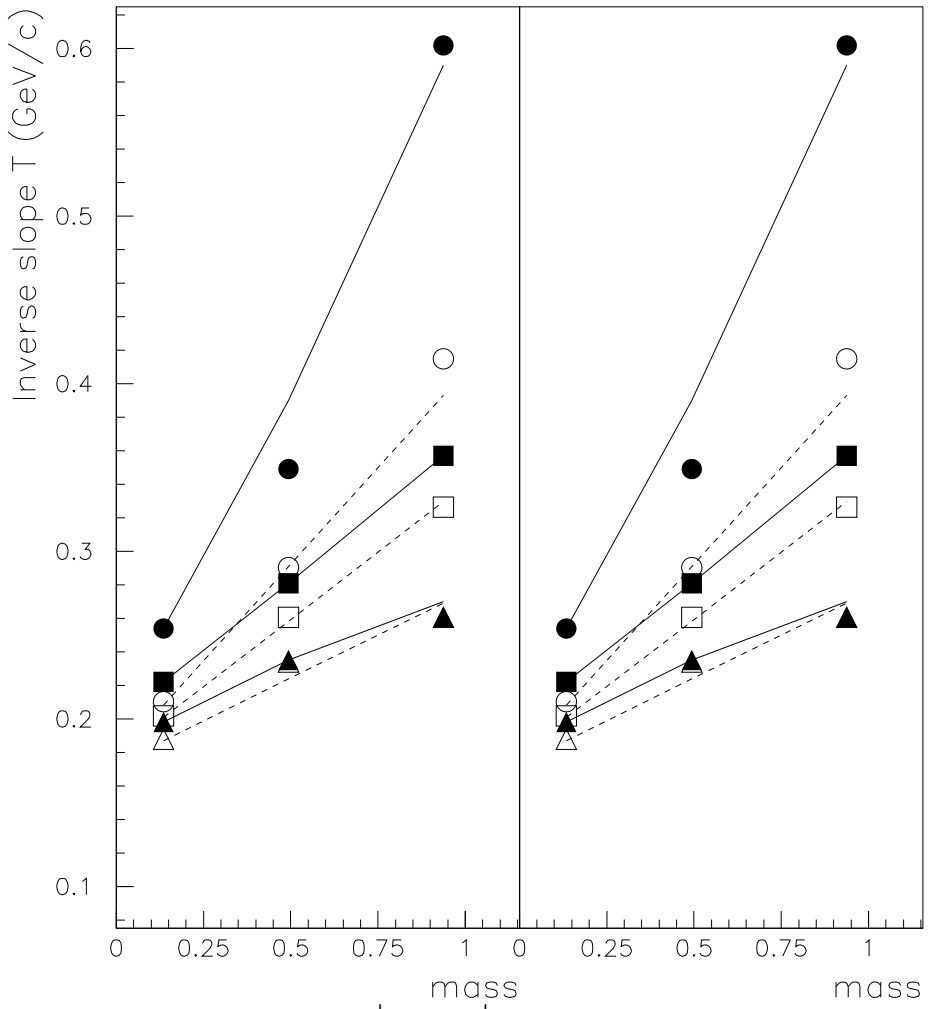

Inverse slope T versus mass for π^+, K^+ and p (left) and π^-, K^- and $\overline{p}$ (right) in three centrality bins for $Au\ Au$ collisions at $\sqrt{s} = 200$ GeV/c. The data points (empty signs) are from PHENIX and the dashed lines are from hydro model. The full signs and full lines are the corresponding values for the initial condition, calculated from our eq. The circles correspond to central, the squares to mid-central and the triangles to peripheral collisions.

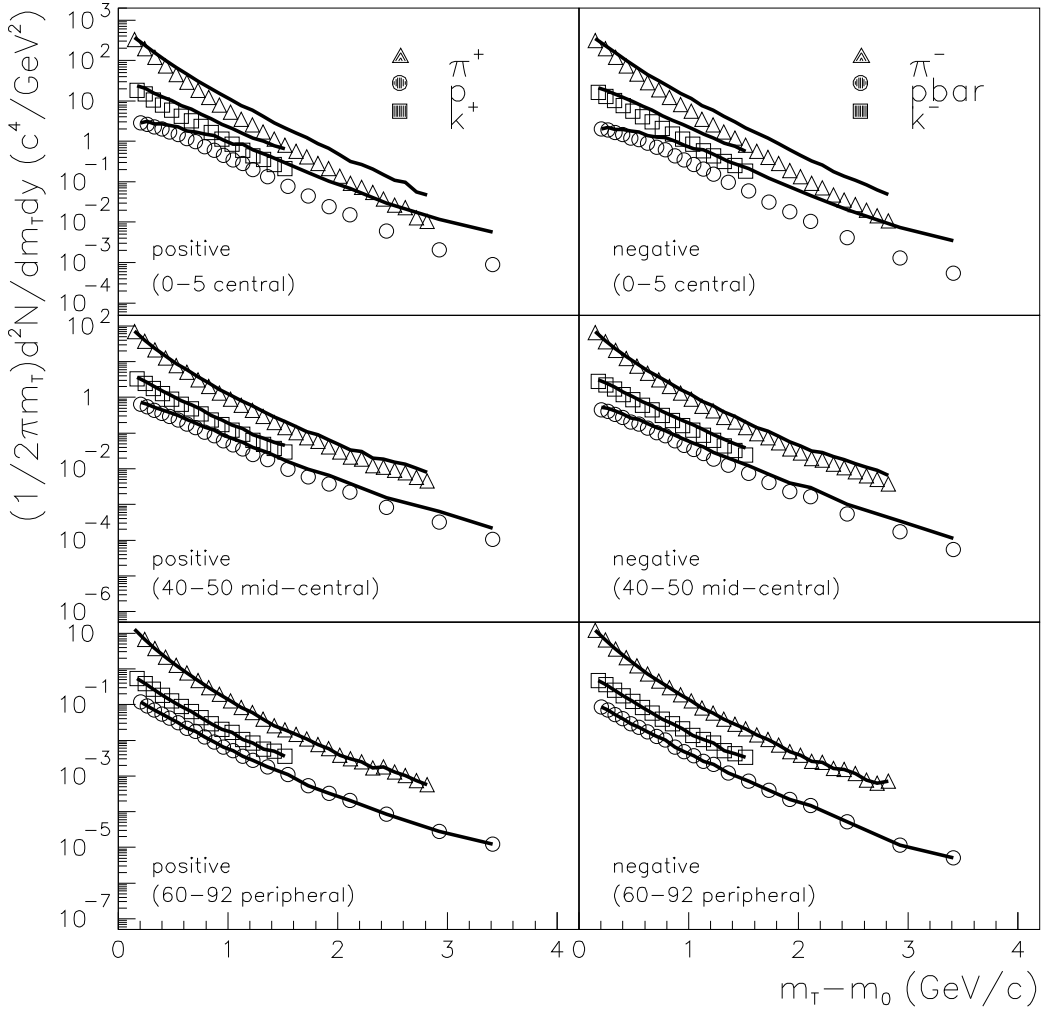

Final (data points) and initial (lines) transverse mass distributions for π^+, K^+ and p (left) and π^-, K^- and $\overline{p}$ (right) in three centrality bins for $Au\ Au$ collisions at $\sqrt{s} = 200$ GeV. The data are from PHENIX. The lines are calculated using our eq. and correspond to the initial condition. As expected, the effect of the final state interaction is important for central collisions and negligibly small for the most peripheral ones.

CONCLUSIONS

The large observed anisotropy at RHIC is argued to be indicative of early local thermal equilibrium, and the particle mass dependence is highly relevant to interpretations involving a strongly interacting Quark Gluon Plasma phase. At larger transverse momenta, measurements of azimuthal anisotropy are also relevant to the observation of jet quenching.

In high energy heavy-ion collisions, a high density system consisting of deconfined quarks and gluons is expected to be created. Energetic partons, resulting from initial hard scatterings, are predicted to lose energy by induced gluon radiation when propagating through the medium. This energy loss is expected to depend strongly on the color charge density of the created system and the traversed path length of the propagating parton.

At Brookhaven s Relativistic Heavy Ion Collider (RHIC) three different observations related to parton energy loss have emerged: strong suppression of the inclusive hadron production, strong suppression of the back-to-back high-pt jet-like correlation, and large values of the elliptic flow at high pt.

In non-central heavy ion collisions, the geometrical overlap region has an almond shape in the transverse plane, with its short axis in the reaction

plane. Depending on the emission azimuthal angle, partons traversing this system, on average, experience different path lengths and therefore different energy loss. It leads to (a) azimuthal anisotropy in high pt particle production with respect to the reaction plane (the second harmonic in the particle azimuthal distribution, elliptic flow) and (b) to the dependence of the high pt 2-particle back-to-back correlations on the orientation of the pair.

DEFINITIONS

v_2 in our approach=medium dependent v_2 en other approaches= gradient of the medium

KOLB The obvious geometric deformation of the overlap region can be quantified by the spatial eccentricity.

OLLI The observation of azimuthal anisotropy in the produc- tion of particles in ultra-relativistic nucleus-nucleus col- isions, especially the so-called elliptic flow v2 [1], is one of the highlights of the RHIC heavy ion program [2, 3]. The phenomenon, first identified in this regime at the CERN SPS [4], reflects the anisotropy of the region of overlap of the nuclei and is a direct consequence of the reinteractions between the produced particles. In the imit where the collisions are frequent enough to drive the system quickly to local equilibrium, fluid dynamics provides an intuitive physical explanation for the origin of anisotropic flow: particles tend to go in the direction of the strongest pressure gradients, hence preferably in the collision plane [5]. Of course, local equilibrium is not a necessary condition for elliptic flow, but it is commonly accepted that deviation from equilibrium can only reduce the magnitude of the e ect.

OLLI To summarize, relaxing the constraint of chemical equi- librium allows for a natural explanation of RHIC data on elliptic flow. Deviations from local equilibrium lead to a characteristic dependence of observables such as v2/ and v4/v2 2 on the number of collisions, and this can be tested experimentally.

DREES The dense medium created in Au + Au collisions at the Relativistic Heavy-Ion Collider (RHIC) significantly suppresses particle production from hard scattering processes and their characteristic back-to-back angular correlation. We present a simple model of jet absorption in dense matter which incorporates a realistic nuclear geometry. Our calculations are performed at the jet level and assume independent jet fragmentation in the vacuum. This model describes quantitatively the centrality dependence of the observed suppression of the high pT hadron yield and of the back-to-back angular correlations. The azimuthal anisotropy of high pT particle production can not be accounted for using a realistic nuclear geometry.

DREES The amount of medium a hard scattered parton traverses, and subsequently its energy loss, varies with the centrality of the collision and also the azimuthal angle with respect to the reaction plane. If the parton energy loss is large, the surviving partons will be emitted dominantly near

the outer layer of the overlap region. The partons moving towards the surface (near side) traverse on average less material than those going in opposite direction (away side). Thus partons scattered to the near side are likely to escape with little energy loss, while the away side partons are likely to lose significant energy and thus are suppressed more strongly.

DREES Due to the asymmetry of the overlap region of the two nuclei, the average amount of matter traversed by a parton depends on its azimuthal direction with respect to the reaction plane, which leads to an azimuthal anisotropy of the emitted jets. This anisotropy reaches its maximum for collisions with an impact parameter of about 9 fm corresponding to approximately 100 participants. It is small for peripheral and central collisions. Our calculation reproduces the measured trend of the centrality dependence of v2, but the magnitude is below the measured value 4. With a matter density profile deduced from a Woods-Saxon distribution, a large fraction of the surviving jets is emitted from the low density region at large radii (see Fig. 2b). Therefore the anisotropy is diluted.

DREES We find that observables like DAA and v2 are more sensitive to the absorption patterns. Our model does not describe v2 quantitatively unless an unrealistic nuclear density profile is used. This might indicate

that the ac- tual di useness of the opaque medium is smaller than expected from the density profile obtained by convolut- ing twoWoods-Saxon nuclear distributions [19]. It is also conceivable that the real suppression is larger, and that the observed suppression is reduced by soft particles from dynamic mechanisms di erent from jet fragmenta- tion, such as hydrodynamics [48] plus viscosity correc- tion [49], quark coalescence [47], and quark/diquark pick up [24]. In this case, both the soft particles and a stronger suppression would lead to a larger v2.

PHENIX0411040 correlation measurements are important in several ways. They serve as a barometric sensor for pressure gradients developed in the collision and hence yield insight into crucial issues of thermalization and the equation of state (EOS) [6, 7, 8]. They provide important constraints for the density of the medium and the e ective energy loss of partons which traverse it [9, 10]. They can provide valuable information on the gluon saturation scale in the nucleus [11]. Recent measurements at RHIC (s = 130 and

PHENIX0411040 Evidence for parton energy loss and jet quenching in the produced medium [3].

PHENIX0411040 At low pT (pT ¡¡ 2.0 GeV/c) the magnitude and trends

of v2 are under-predicted by hadronic cascade models supplemented with string dynamics [21], but are well reproduced by models which incorporate hydrodynamic flow [5, 7]. This has been interpreted as evidence for the production of a thermalized state of partonic matter [3, 4, 5]. At higher pT the predictions of quark coalescence [22] are consistent with the data [20, 23], and quantitative agreement has been achieved with transport model calculations which incorporate large opacities [10].

PHENIX0411040 Three analysis methods: analysis. In the first, we used the reaction plane technique which correlates the azimuthal angles of charged tracks detected in the central arms with the azimuth of an estimated event plane 2, determined via hits in the North and South BBC s located at —¡ 3 3.9 [20]. In the second method, a cumulant analysis was performed on data collected at sNN = 200 and 62.4 GeV to obtain the anisotropy directly [31] In the third method, we extracted the anisotropy at sNN = 62.4, 130 and 200 GeV via assorted two-particle correlation functions [12, 20]

One of the largest uncertainties in elliptic flow measurements in nuclear collisions is due to so-called non-flow effects the contribution to the azimuthal correlations not related to the reaction plane orientation, such as

resonance decays and inter- and intra-jet correlations.

STAR0407007 Although results presented above strongly support the jet-quenching scenario qualitatively, the amount of ellip- tic flow observed at high pt for collisions at sNN= 130 GeV seems to exceed the values expected in the case of complete quenching [23]. Extreme quenching leads to emission of high-pt particles predominantly from the sur- face, and in this case v2 would be fully determined by the geometry of the collision. This hypothesis can be tested by studying the centrality dependence of v2 for high-pt particles.

Figure 4 shows v2 in the pt-range of 3 6 GeV/c (where v2 is approximately maximal and constant) versus impact parameter. The values of the impact parameters were ob- ained using a Monte Carlo Glauber calculation [24]. The measured values of v24 are compared to various simple models of jet quenching. The upper curve corresponds to a complete quenching, in which particles are emitted from a hard shell [23, 25]; this gives the maximum values of v2 hat are possible in a surface emission scenario. A more ealistic calculation corresponds to a parameterization of et energy loss in a static medium where the absorption coe cient is set to match the suppression of the inclu- ive hadron yields [5]. The density distributions of the

PHENIX0305013 A striking feature observed at higher pT is that the v2 of p and p are larger than for and K at pT ¿ 2 GeV/c. This is in sharp contrast to the hydrodynamical picture, which would predict the same mass-ordering for v2 at all pT. In our data the mesons begin to show a departure from the hydrodynamical prediction at pT of about 1.5 GeV/c, while the (anti)baryons agree with the prediction up until 3 GeV/c but may be deviating at higher pT. Such behavior is predicted by the quark coalescence mechanism in which the anisotropy of the final-state hadrons is largely inherited from the anisotropy of quarks in a preceding quark-matter phase.

CONCLUSIONS

Together with previous work on strangeness enhancement, J/ψ suppression and fixed p_T suppression, all of which can be described in our framework with final state interaction cross-section smaller than or of the order of 2 mb, this work lends support to the idea that, despite the large densities reached in central $Au\ Au$ collisions, the final state interaction is rather weak. In terms of string models, it means that there is "cross-talk" between different strings. However, the concept of string remains useful and these models can be used to compute the densities needed as initial conditions in the gain and loss differential equations which govern the final state interaction. Such a weak cross-talk, in the presence of many strings per unit of transverse are, is supported theoretically by the small transverse size of the string – with a radius of the order of 0.1 fm. On the experimental side it is supported by the nuclear transparency of proton-nucleus collisions – where no "cross-talk" is needed to reproduce the data. As a consequence, only rear events are substantially affec ted but the bulk of the system is not – indicating that the strength and duration time of the final state interaction are not enough to drive the system to thermal equilibration.

DETAILS

Multiplicies: Shadowing corrections

$$\frac{dN_{AA}}{dy}(b) = a(y,b)N_{part}(b) + c(y,b)N_{coll}(b).$$

A) $N_{part}(b) \propto A$: number of participant nucleons, valence-like contribution.
B) $N_{coll}(b) \propto A^{4/3}$: number of inelastic nucleon-nucleon collisions (not only hard), dominant at asymptotic energies.

To get the right multiplicities at RHIC, some mechanisms to lower the contribution of B) have been introduced:

- Very strong shadowing of gluon distributions in nuclei in HIJING (S.-Y.Li)
- Geometrical parton saturation (K.J.Eskola et al)
- Pomeron interaction in DPM (A.Capella et al.)
- Saturation in high-density QCD: CGC (D.E.Kharzeev et al.)
- Interaction/percolation of strings (C. Pajares et al.)

All these mechanisms have in common the presence and/or modification of a multiple scattering pattern (in the target rest frame) or gluon interaction (in a fast moving frame).

Shadowing corrections

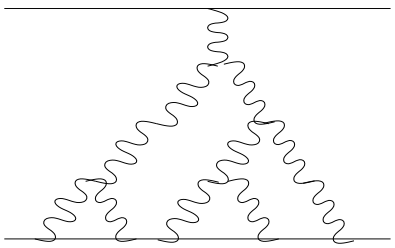

Our approach contains dynamical, non linear shadowing
It is determined in terms of diffractive cross sections
It would lead to saturation at $s \longrightarrow \infty$
Controled by triple pomeron diagrams

Reduction of multiplicity from shadowing corrections:

$$R_{AB}(b) = \frac{\int d^2s f_A(s) f_B(b-s)}{T_{AB}(s)}, \quad f_A(b) = \frac{T_A(b)}{1 + AF(s)T_A(b)}$$

Function F: Integral of the triple P cross section over the single P one:

$$F(s) = 4\pi \int_{y_{min}}^{y_{max}} dy \frac{1}{\sigma^P(s)} \frac{d^2\sigma^{PPP}}{dydt}|_{t=0} = C[\exp(\mathrm{y_{max}}) - \exp(y_{min})]$$

$y = \ln(s/M^2)$, $M^2 =$ squared mass of the diffractive system

Particle produced at $y = 0 \Rightarrow$
$y_{max} = \frac{1}{2}\ln(s/m_T^2)$, $y_{min} = \ln(R_A m_N/\sqrt{3})$, $C =$ triple pomeron coupling

At large p_T: Shadowing decrease due to the increase of m_T in y_{max}

Due to coherence conditions, shadowing effects for partons take place at very small x, $x \ll x_{cr} = 1/m_N R_A$ where m_N is the nucleon mass and R_A is the radius of the nucleus.

Partons which produce a state with transverse mass m_T and a given value of Feynman x_F, have $x = x_\pm = \frac{1}{2}(\sqrt{x_F^2 + 4m_T^2/s} \pm x_F)$

Our shadowing applies to soft and hard processes. Nevertheless, for large p_T these effects are important only at very high energies, when $x \sim \frac{m_T}{\sqrt{s}}$ satisfies the above condition.

At fixed initial energy (s) the condition for existence of shadowing will not be satisfied at large transverse momenta: In the central rapidity region $(y^* = 0)$ at RHIC and for p_T of jets (particles) above 5(2) GeV/c the condition for shadowing is not satisfied and these effects are absent.

If the triple pomeron coupling is small:

$[1 + AF(s)T_A(b)]^{-1} \sim 1 - AF(s)T_A(b) \Rightarrow$ Only the contribution of the triple P graph is involved in the shadowing

If the triple pomeron coupling is large:

One needs to sum all of fan diagrams with Pomeron branchings (Schwimmer model) $\Rightarrow [1 + AF(s)T_A(b)]^{-1}$

In the limit of large triple pomeron coupling:

$[1 + AF(s)T_A(b)]^{-1} \sim [AF(s)T_A(b)]^{-1}$

A-dependence: $\frac{dN_{AA}}{dy} \sim A^{4/3}$ changes to $\frac{dN_{AA}}{dy} \sim A^{2/3}$

Our result for AA at RHIC energies: $\frac{dN_{AA}}{dy} \sim A^{1.13}$

Comparison with the saturation model

In the saturation regime ($\Lambda_{QCD} << p_T < Q_s$:)

$$\frac{dN}{dyd^2p_T} \sim \frac{A^{2/3}}{\alpha_s(Q_s^2)}$$

Same result as for maximal shadowing

First correction: Integrating over d^2p_T up to Q_s and assuming a p_T broadening corresponding to $Q_s^2 \sim A^{1/3}$:

$$\frac{dN}{dy} \sim xG(x,Q_s^2) = \frac{\pi R_A^2\, Q_s^2(x,A)}{\alpha_s(Q_s^2)} \sim \frac{A}{\alpha_s(Q_s^2)}$$

Second correction: $\alpha_s^{-1}(Q_s^2) \sim logA^{1/3}$

Problem: a p_T broadening in $A^{1/3}$ is too large

Third correction: $\alpha_s^{-1} \sim log[(0.61 + 0.39(\frac{N_{part}(b)}{N_{part_{max}}})^{1/3})/0.6]$

b (fm)	$Shadow$
0	0.656
2	0.657
4	0.664
6	0.681
8	0.712
10	0.763
12	0.843

Shadowing corrections, integrated over p_T, for Au+Au collisions at RHIC

Diffraction

The total cross section:

$$\begin{aligned}
\sigma_{tot}(x,Q^2) &= \int_0^{r_0} d^2r \int_0^1 d\alpha \, |\Psi^{T,L}_{\gamma^* q}(\alpha,r)|^2 \, \sigma^{dipole}_{CFKS}(x,r) \\
\sigma^{dipole}_{CFKS}(x,r) &= 4 \int d^2b \; \sigma^{n\,I\!P}(x,Q^2,b,r) \\
\sigma^{n\,I\!P}(x,Q^2,b,r) &\simeq 1 - \exp[-\, r^2 \chi^{n\,I\!P}(x,Q^2,b)\,]
\end{aligned}$$

Single Pomeron exchange amplitude:

$$\chi^{I\!P}(s,b,Q^2) \simeq \frac{C_{I\!P}}{R(x,Q^2)} \left(\frac{Q^2}{s_0+Q^2} \right)^{\varepsilon_{I\!P}} x^{-\varepsilon_{I\!P}} \exp[-b^2/R(x,Q^2)] \, .$$

The resummation of the triple-Pomeron branches is encoded in the denominator of the amplitude $\chi^{n\,I\!P}$, i.e. the Born term in the eikonal expansion.

$$\chi^{n\,I\!P}(x,Q^2,b) = \frac{\chi^{I\!P}(x,Q^2,b)}{1+a\chi_3(x,Q^2,b)}$$

where the constant a depends on the proton-Pomeron and the triple-Pomeron couplings at zero momentum transfer ($t=0$).

Diffractive cross section:

$$\sigma_{diff}(x,Q^2) = 4 \int d^2b (\sigma_{tot}(b,x,Q^2))^2$$

We assume longitudinal boost invariance. Therefore, the above picture is not valid in the fragmentation regions.

We assume that the dilution in time of the densities is only due to longitudinal motion: Transverse expansion is neglected. The fact that HBT radii are similar at SPS and RHIC and of the order of magnitude of the nuclear radii, seems to indicate that this expansion is not large. The effect of a small transverse expansion can presumably be taken into account by a small change of the final state interaction cross-section.

The logarithmic factor in Eq. 3 is the result of an integration in the proper time τ from the initial time to freeze-out time. (One assumes a decrease of densities with proper time in $1/\tau$.) A large contribution to this integral comes from the few first fm/c after the collision – where the system is in a pre-hadronic stage. Actually, Brodsky and Mueller introduced the comover interaction as a coalescence phenomenon at the partonic level.

At RHIC $N_{pp}(0) = 2.24$ fm^{-2}. This density is about 90 % larger than at SPS energies. Since the corresponding increase in the AA density is comparable, the average duration time of the interaction will be approximately the same at CERN-SPS and RHIC, about 5 to 7 fm.

Derivation of the suppression factor S_{π^0}

Gain and loss diferential equation for pions:

$$\frac{d\rho_{\pi^0}(x,p_T)}{d^4x} = -\widetilde{\sigma}\ \rho_{medium}\left[\rho_{\pi^0}(x,p_T) - \rho_{\pi^0}(x,p_T+\delta p_T)\right]$$

This is equivalet to the loss equation for the J/ψ suppression due to its interaction with comovers:

$$\frac{d\rho_{J/\psi}(x)}{d^4x} = -\sigma_{co}\ \rho_h(x)\rho_{J/\psi}(x),\ \text{where } dx^4 = \tau d\tau dy ds^2$$

Since $\rho(\tau,y,s) = \rho(y,s)\frac{\tau_0}{\tau}$ –dilution on time of densities–:

$$\frac{\tau d\rho_{\pi^0}}{d\tau} = -\widetilde{\sigma}\ \rho_{medium}\ \rho_{\pi^0}(b,s,y,p_T) + \widetilde{\sigma}\ \rho_{medium}\ \rho_{\pi^0}(b,s,y,p_T+\delta p_T)$$

Putting $\rho(y,s,b) = dN/dyds^2db$, we obtain:

$$\tau\,\frac{dN_{\pi^0}(b,s,y,p_T)}{d\tau} = -\widetilde{\sigma}N_{medium}(b,s,y)N_{\pi^0}(b,s,y,p_T)\left[1-\frac{N_{\pi^0}(b,s,y,p_T+\delta p_T)}{N_{\pi^0}(b,s,y,p_T)}\right]$$

$$dN_{\pi^0}(b,s,y,p_T) = -\widetilde{\sigma}N_{medium}(b,s,y)N_{\pi^0}(b,s,y,p_T)\left[1-\frac{N_{\pi^0}(b,s,y,p_T+\delta p_T)}{N_{\pi^0}(b,s,y,p_T)}\right]\frac{d\tau}{\tau}$$

After integration:

$$N_{\pi^0}(b,s,y,p_T)|_{\tau_f} - N_{\pi^0}(b,s,y,p_T)|_{\tau_0} =$$

$$-\widetilde{\sigma}N(b,s,y)N_{\pi^0}(b,s,y,p_T)\left[1-\frac{N_{\pi^0}(b,s,y,p_T+\delta p_T)}{N_{\pi^0}(b,s,y,p_T)}\right]\ell n\left(\frac{\tau_f}{\tau_0}\right)$$

All densities in the r.h.s. are at initial time, τ_0, so:

$$N_{\pi^0}(b,s,y,p_T)|_{\tau_f} =$$

$$N_{\pi^0}(b,s,y,p_T)_{\tau_0}\left[1-\widetilde{\sigma}\left[1-\frac{N_{\pi^0}(b,s,y,p_T+\delta p_T)}{N_{\pi^0}(b,s,y,p_T)}\right]N(b,s,y)\ell n\left(\frac{\tau_f}{\tau_0}\right)\right]$$

and for a finite formation time,

$$N_{\pi^0}(b,s,y,p_T)|_{\tau_f} =$$

$$N_{\pi^0}(b,s,y,p_T)_{\tau_0} \exp\left\{-\widetilde{\sigma}\left[1-\frac{N_{\pi^0}(b,s,y,p_T+\delta p_T)}{N_{\pi^0}(b,s,y,p_T)}\right] N(b,s,y)\ell n\left(\frac{\tau_f}{\tau_0}\right)\right\}$$

$$= N_{\pi^0}(b,s,y,p_T)_{\tau_0}\widetilde{S}\ ,$$

where the suppression factor is:

$$\widetilde{S}_{\pi^0}(b,s,y,p_T) = \exp\left\{-\widetilde{\sigma}\left[1-\frac{N_{\pi^0}(b,s,y,p_T+\delta p_T)}{N_{\pi^0}(b,s,y,p_T)}\right] N(b,s,y)\ell n\left(\frac{\tau_f}{\tau_0}\right)\right\}\ .$$

Since $N \sim 1/\tau \Rightarrow \tau_f = 1/N_f = 1/N_{pp}$, $\tau_0 = 1/N(b,s,y) = 1/N_{medium}$

$$\widetilde{S}_{\pi^0}(b,s,y,p_T) = \exp\left\{-\widetilde{\sigma}\left[1-\frac{N_{\pi^0}(b,s,y,p_T+\delta p_T)}{N_{\pi^0}(b,s,y,p_T)}\right] N(b,s,y)\ell n\left(\frac{N(b,s,y)}{N_{pp}(y)}\right)\right\}\ .$$

p_T	I	II	III	IV	V	VI	VII
0.5	0.38	0.05			0.34	0.38	0.38
2	0.90	0.13	0.08	0.11	0.20	0.31	0.31
5	1.48	0.21	0.18	0.19	0.23	0.25	0.25
7	1.69	0.24	0.24	0.24	0.24	0.24	0.24
10	1.84	0.27	0.34	0.30	0.25	0.24	0.32

Values of $R^{\pi^0}_{AuAu}(p_T)$ for the 10 % most central $AuAu$ collisions at $\sqrt{\mathbf{s}_{NN}} = 200$ GeV and at mid-rapidities ($|y^*| < 0.35$).

Column I is the result obtained with no final state interaction.

Column II is the result obtained with final state interaction neglecting the shift.

Column III and IV is the result obtained with final state interaction introducing the shift as $\delta p_T = 0.5$ GeV/c and $\delta p_T = 1.5$ GeV/c.

Column V is the result obtained with final state interaction introducing the shift as $\delta p_T = (p_T - < p_T >_b)/20$.

Column VI is the result obtained with final state interaction introducing the shift as $\delta p_T = (p_T - < p_T >_b)^{1.5}/20$.

Column VII is the result obtained with final state interaction introducing the shift as $\delta p_T = (p_T - < p_T >_b)^{1.5}/20$ for $p_T < 7$ GeV/c and $\delta p_T = (7 - < p_T >_b)/20$ for $p > 7$ GeV/c.

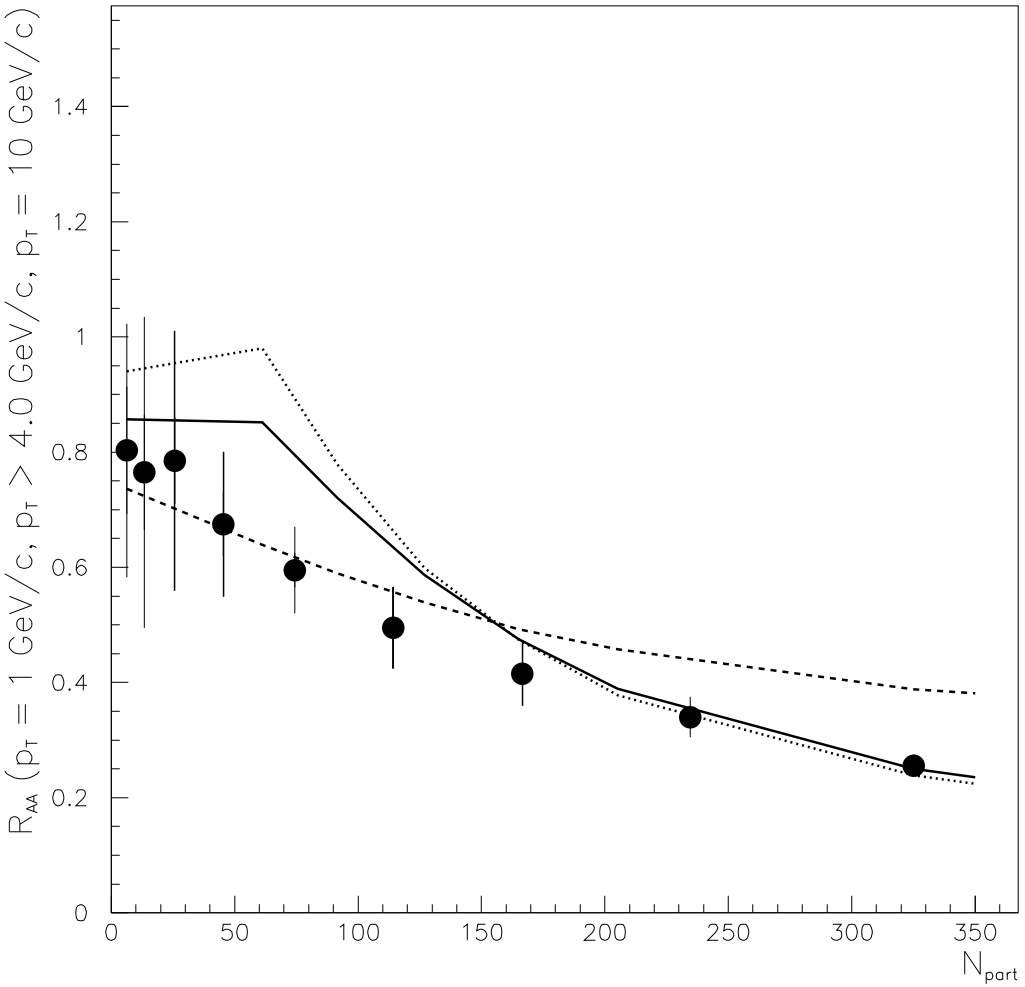

Centrality dependence of $R^{\pi^0}_{AuAu}$ for $p_T > 4$ GeV/c, $p_T = 1$ GeV/c and $p_T = 10$ GeV/c using the p_T shift $\delta p_T = (p_T - < p_T >_b)^{1.5}/20$. The data are from PHENIX.

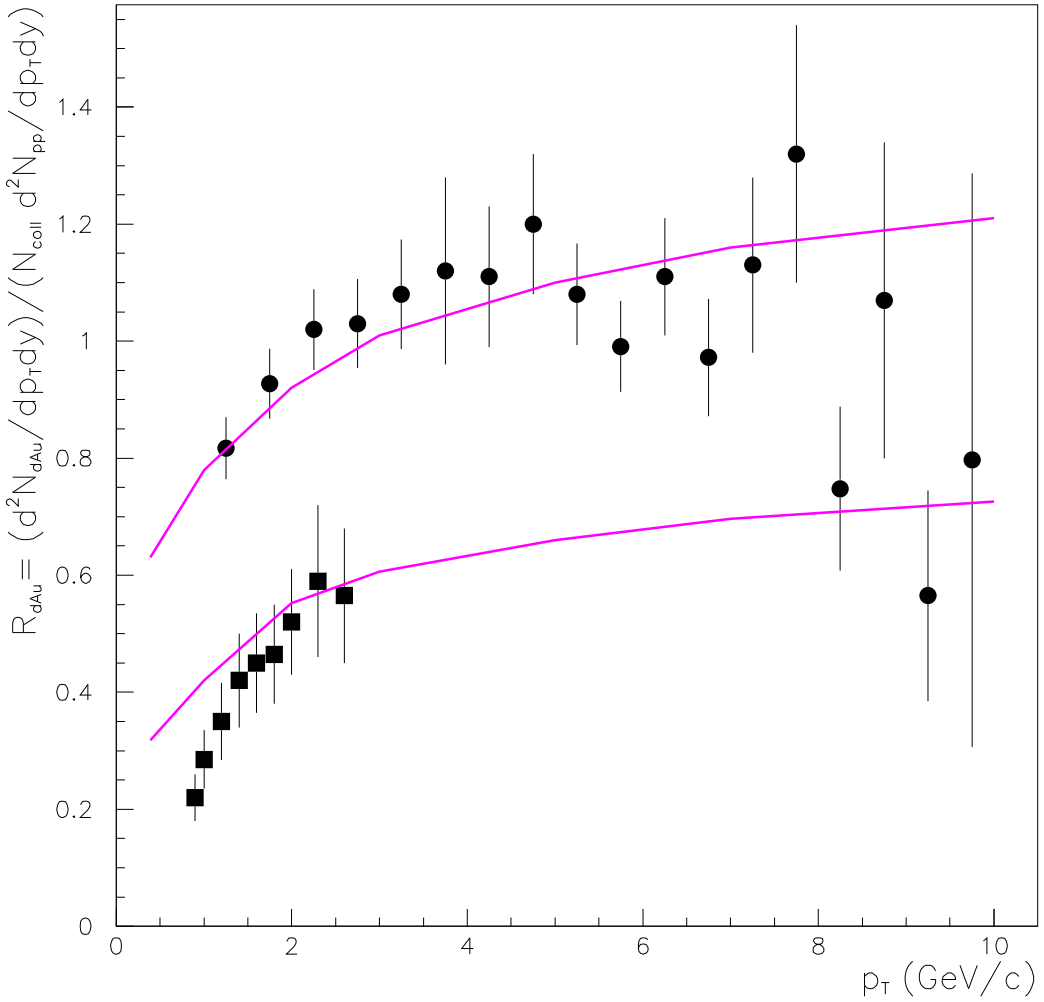
$R_{dAu} = (d^2N_{dAu}/dp_T dy)/(N_{coll}\ d^2N_{pp}/dp_T dy)$
0
0.2
0.4
0.6
0.8
1
1.2
1.4
0
2
4
6
8
10
p_T (GeV/c)

OPEN QUESTIONS

What is the correct treatment of the energy loss? Should we use the perturbative approach or nonperturbative processes with small momentum transfer are dominant?

Should the suppression effect decrease as p_T increases? Note that these secondary reinteractions violate QCD factorization theorem.

What is the correct transition from coherent (shadowing) to non- coherent region?

Is the formula for interaction with comovers than we are using reasonable for large p_T?

Where are the effects of suppression due to nuclear absorption? At large p_T, nuclear absorption is expected to be present both in dAu and $AuAu$ collisions. The dAu data at large p_T are consistent with the presence of nuclear absorption. However, the error bars are too large in order to perform a quantitative study of this question – and determine the value of σ_{abs}. Introducing nuclear absorption in $AuAu$ collisions would result in a smaller value of $\widetilde{\sigma}$.